nature portfolio

https://doi.org/10.1038/s41586-024-07426-9

## Supplementary information

# Adhesive anti-fibrotic interfaces on diverse organs

In the format provided by the authors and unedited

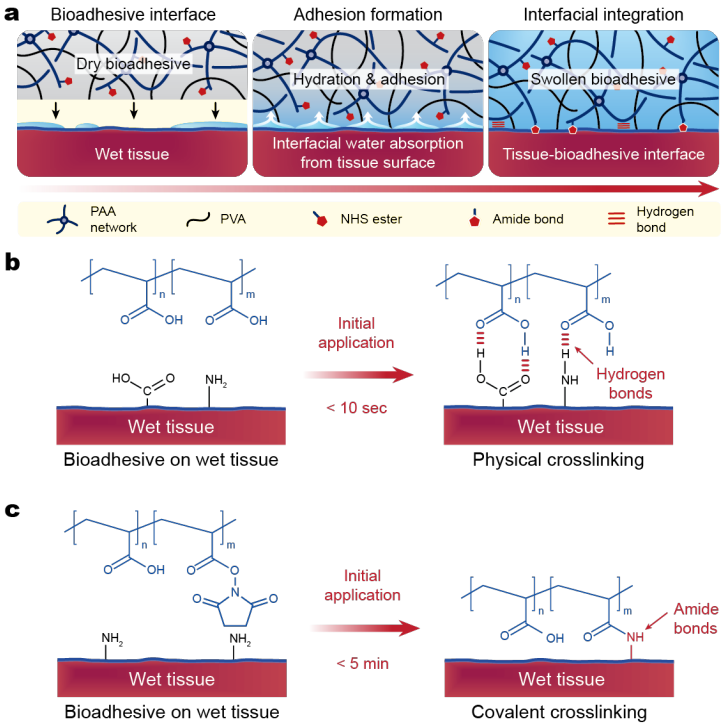


**Supplementary Fig. 1 | Adhesion mechanism and chemistry of the adhesive implant. a**, Schematic illustrations for adhesion of the adhesive implant to wet tissues. **b**, Schematic illustrations for physical crosslinking between the adhesive implant and the tissue by hydrogen bonds. **c**, Schematic illustrations for covalent crosslinking between the adhesive implant and the tissue by amide bonds.

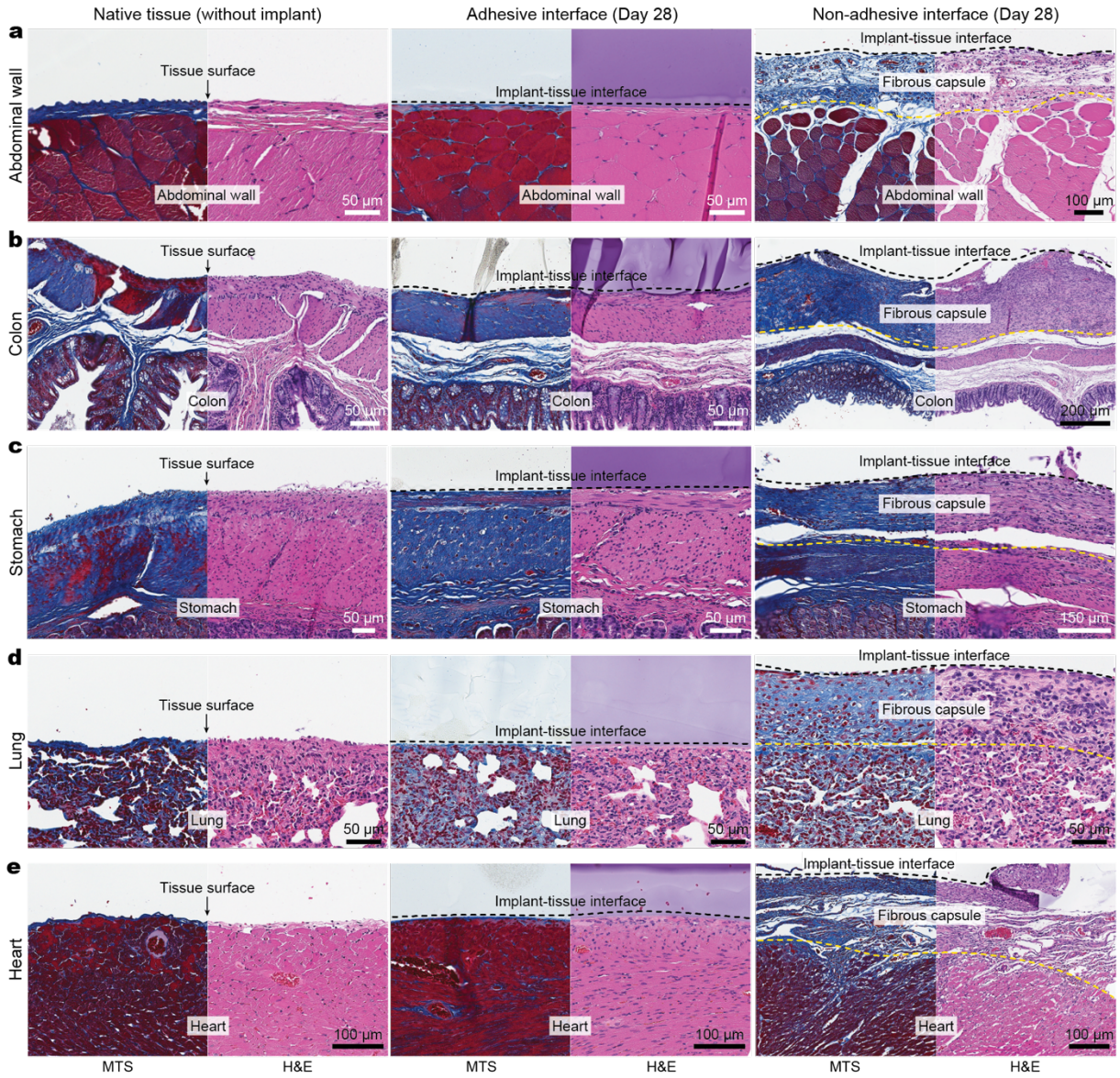


**Supplementary Fig. 2 | Adhesive implant-tissue interface on diverse organs. a-e**, Representative histology images stained with Masson's trichrome (MTS) and hematoxylin and eosin (H&E) for native tissue (left), adhesive implant (middle), and non-adhesive implant (right) collected on day 28 post-implantation to the abdominal wall (a), colon (b), stomach (c), lung (d), and heart (e). Black and yellow dotted lines in the images indicate the implant-tissue interface and the fibrous capsule-tissue interface, respectively. The experiment was repeated independently ($n$ = 4 per group) with similar results.

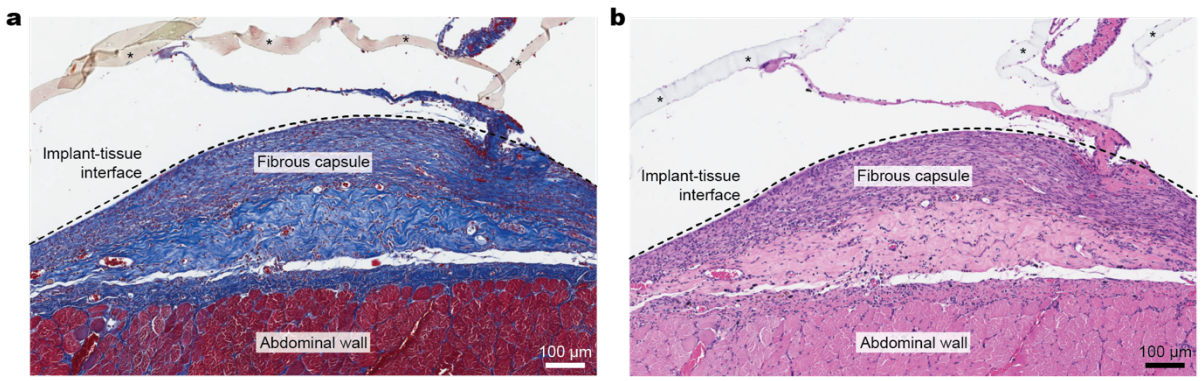


**Supplementary Fig. 3 | Polyurethane mock device. a**,**b**, Representative histology images stained with Masson's trichrome (a) and hematoxylin and eosin (b) of the polyurethane mock device collected on day 28 post-implantation to the abdominal wall. * in images indicates the implant; black dotted lines indicate the implant-tissue interface. The experiment was repeated independently ($n = 4$) with similar results.

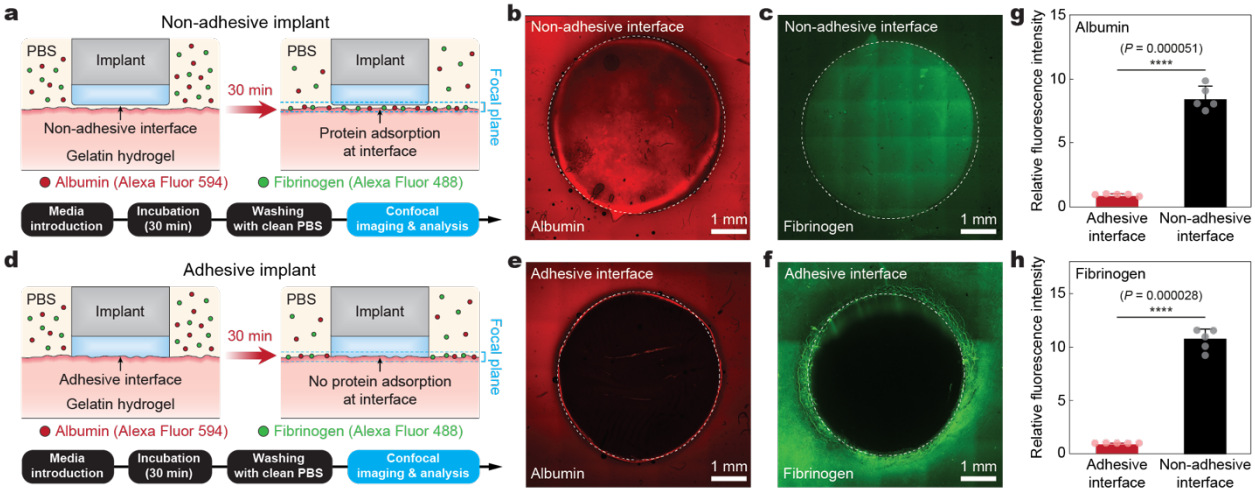


**Supplementary Fig. 4 | In vitro protein adsorption assay. a-c**, Schematic illustration of the experimental setup (a) and representative confocal microscope images for in vitro albumin (b) and fibrinogen (c) adsorption assay for the non-adhesive implant. **d-f**, Schematic illustration of the experimental setup (d) and representative confocal microscope images for in vitro albumin (e) and fibrinogen (f) adsorption assay for the adhesive implant. **g**,**h**, Relative fluorescence intensity at the implant-substrate interface measured 30 min after co-culture for albumin (g) and fibrinogen (h). Values in **g**,**h** represent the mean and the standard deviation ($n = 5$; independent samples). Statistical significance and $P$ values are determined by two-sided unpaired $t$-tests; $^{****}P < 0.0001$.

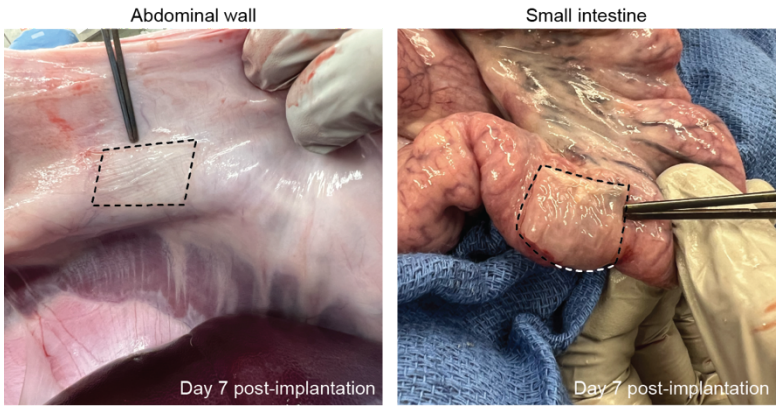


**Supplementary Fig. 5 l In vivo implantation of the adhesive implants on porcine organs.** Photographs of the porcine abdominal wall and small intestine on day 7 post-implantation for the adhesive implant. Black dotted lines in photographs indicate the boundary of implants.

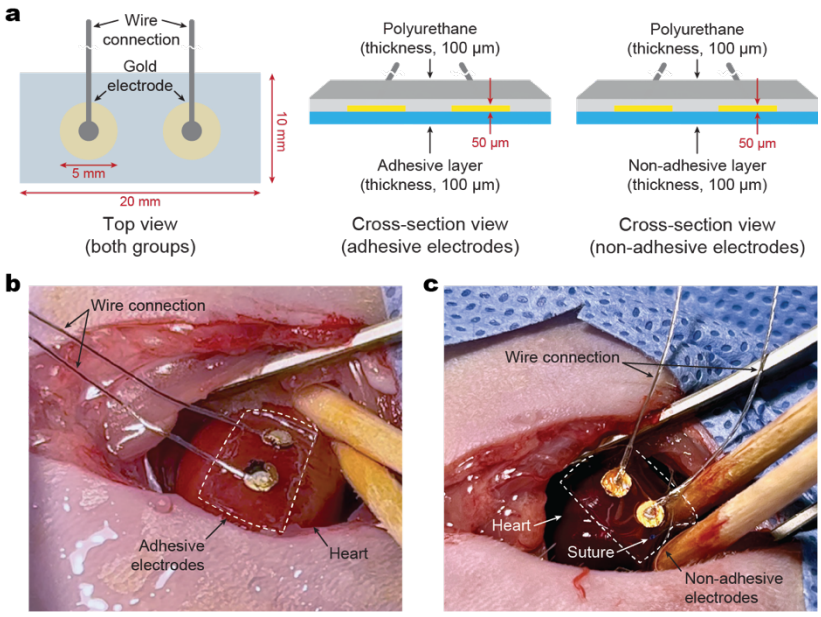


**Supplementary Fig. 6 | Electrodes with the adhesive and non-adhesive interfaces. a**, Schematic illustrations for electrodes with the adhesive and the non-adhesive interfaces. **b**,**c**, Photographs of electrodes with the adhesive interface (b) and the non-adhesive interface (c) implanted to the rat epicardial surface. White dotted lines in photographs indicate the boundary of implants.

**Supplementary Table 1 | Luminex multiplex assays for protein profiling of rat abdominal wall tissues.** Data were normalized per total amount of proteins extracted and are represented as the mean ± standard deviation ($n$ = 3 tissue lysates; independent biological replicates). Statistical significance and $P$ values are determined by two-sided unpaired $t$-tests; *$P < 0.05$ (vs. non-adhesive interface for the same time point).

| Molecule (pg $mg^{-1}$ protein) | Non-adhesive interface | | Adhesive interface | |
|---|---|---|---|---|
| | Day 3 | Day 7 | Day 3 | Day 7 |
| IL-1α | 6.87±2.61 | 10.47±5.38 | 3.87±0.45 | 8.75±5.08 |
| IL-1β | 107.65±129.51 | 125.97±130.24 | 20.95±4 | 26.77±8.04 |
| IL-6 | 31.48±45.88 | 50.44±60 | 15.31±11.07 | 18.74±6.33 |
| IL-12P70 | 1.05±0.23 | 1.18±0.32 | 1.74±0.28* | 1.7±0.35 |
| IL-17 | 3.18±0.34 | 4.04±1.2 | 3.22±0.47 | 3.74±0.2 |
| IL-18 | 394.21±20.14 | 430.18±111.11 | 192.43±28.83* | 145.5±12.14* |
| TNF-α | 0.58±0.02 | 0.98±0.4 | 0.69±0.07 | 0.65±0.11 |
| MCP-1 | 53.77±44.43 | 64.64±28.67 | 47.47±16.12 | 34.17±2.23 |
| G-CSF | 0.2±0.05 | 0.25±0.03 | 0.36±0.06* | 0.34±0.06 |
| IL-4 | 12.62±5.8 | 12.61±1.71 | 17.41±3.46 | 13.13±1.61 |
| IL-10 | 4.64±2.63 | 9.93±11.36 | 3.03±0.35 | 2.31±0.25 |
| CCL3 | 17.34±3.56 | 77.24±73.93 | 9.21±1.15* | 20.74±14.28 |
| CCL5 | 10.15±1.49 | 69.24±31.03 | 5.88±0.84* | 38.57±25.39 |

**Supplementary Table 2 | Mechanical properties of the implants in this study**

| Implant | Young's modulus | Thickness |
|---|---|---|
| Polyurethane | 2.1 MPa | 100 $\mu$m |
| Gold electrode | 79 GPa | 50 $\mu$m |